The Influence of Plasma Nitriding Technology Parameters on the Hardness of 18ХГТ Steel Parts

Nguyen Thai Van
Vinh Long University of Technology Education, Vietnam
vannt@vlute.edu.vn

Le Hong Ky
Vinh Long University of Technology Education, Vietnam
kylh@vlute.edu.vn (corresponding author)

Received: 17 February 2024 | Revised: 4 March 2024 | Accepted: 5 March 2024

 DOI: https://doi.org/10.48084/etasr.7089

ABSTRACT

This article presents the results of the research on the influence of plasma nitriding technology parameters on the working surface hardness of machine parts made of previously hardened 18ХГТ steel. A total of 27 experiments were conducted on the H4580 Eltrolab instrument. Minitab software was used to process the experimental results. The regression function set up with visual charts was utilized as the basis for analysis of the influence of temperature, time, and gas permeation concentration on the working surface hardness. Analysis of variance (ANOVA) showed that all the nitriding technology parameters influenced the regression function. The permeation temperature *TL* had the greatest influence on hardness, while the permeation time *h* and the gas permeation concentration *G1* had less influence. When the double interaction between the parameters was considered, it was shown that these pairs also had a large influence on the surface hardness, but at different levels.

Keywords-permeation temperature; permeation time; gas permeation concentration; working surface hardness; plasma nitriding; regression equation

I. INTRODUCTION

A permeable layer with high resistance to wear and corrosion and enhanced fatigue resistance can be created on the surface of a part by plasma nitriding. Plasma nitriding is a surface treatment method that uses nitrogen at low pressure and is commonly applied to machine parts made from steel [1]. The infiltration process is performed in a vacuum furnace at low pressure with a gas mixture, composed of H_2, N_2, CH_4, and Ar. [1, 2]. This technology has the benefit of being able to regulate the diffusion layer, which makes it ideal for infiltrating products that have high quality standards [2]. When the parts are exposed to high voltage, the gases become plasma, a state of matter with charged particles. The nitrogen particles in the plasma gain speed when they collide with the parts' surface. This collision causes heat, cleaning, and the formation of a thin and hard layer that resists wear and improves fatigue strength [3]. The permeable layer quality in the nitriding process model depends on various parameters, which are difficult to measure accurately [4-9]. Many researchers have tried to estimate gas nitriding and plasma nitriding processes [5, 6]. Authors in [10] studied how nitride layers form on pure iron during plasma nitriding. They applied Wagner's generalized common model to explain the permeable layer formation and compared it with the experimental results of plasma nitriding. The predictive models they proposed all follow the rule that the nitrogen content in the permeable layer and the diffusion zone increases in a parabolic way in plasma nitriding [7, 8]. A numerical simulation model for the formation and distribution of nitride layers and nitrogen in the ε, γ', and α phases during plasma nitriding of pure iron was developed in [11]. It was found that the nitride layers are composed of ε, γ', and α phases and that the thickness of each phase grows in a parabolic curve, the same as in previous works [12]. Authors in [13] provided a numerical model of nitrogen diffusion in pure iron, which shows that the diffusion depends on the concentration of nitrogen. They calculated the thickness of the permeable layers to be the square root of the nitriding time at 843 K (570 ^oC) [7]. Authors in [14] used a gas mixture of NH_3-H_2 to permeate the gas and form the nitriding layer. They adopted a well-known model based on Fick's law to examine the growth kinetics of the γ' phase during gas nitriding on pure iron. They also developed a simple model to estimate the thickness of the nitride layers in pure iron and constructed a plasma nitriding model using a kinetic model derived from Fick's second law.

The literature on plasma nitriding is abundant, but there is little research on the formation of nitride compounds in the

plasma nitriding layer. Some methods have been developed to calculate and predict the nitrogen concentration and the nitride compounds produced during the nitriding process for pure iron and to measure the depth of the nitrogen diffusion zone in parts after plasma nitriding [4, 5, 14-17].

We did not find any research on plasma nitriding of 18ХГТ alloy steel parts, especially on hypoid gears. This study uses an ELTROPUL permeation furnace with a pre-generated plasma pulse source that produces stable plasma in all cases and easily penetrates parts with complex geometries.

II. EXPERIMENTAL PART

The passive hypoid gear teeth are made of 18ХГТ steel according to Russian standards (equivalent to ASTM's SAE 5120). The chemical composition of the elements (%) is: C: 0.17-0.23; Si: 0.17-0.37; Mn: 0.8-1.1; P: < 0.035; S: < 0.035; Cr: 1-1.3; Ni: < 0.3; Ti: 0.03-0.09; Cu: < 0.3; and N: < 0.008 [17]. Surface hardness is often understood as the maximum hardness, although the maximum hardness is found usually a few μm from the surface. The penetration layer depth and the hardness (or micro hardness) are inversely related. The teeth, part of the plasma nitriding sample, are separated by wire cutting and are numbered from 1 to 27, see Figure 1(a).

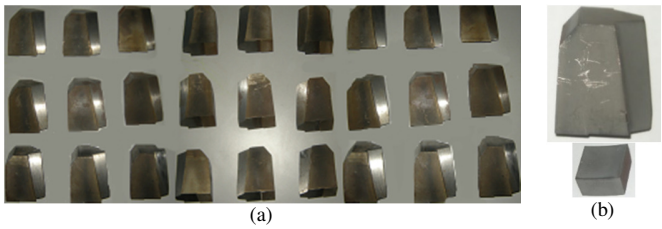

(a) (b)

Fig. 1. Sample preparation. (a) The plasma nitriding sample, (b) experimental samples and control sample.

To compare the working hardness after applying the JIS Z 2244-2009 standard, each experiment considered two samples of the same material: one experimental sample and one control sample. The H4580 Eltrolab instrument was used to perform plasma nitriding with a programmable setting. The permeation process is similar for samples of the same material and size, so the voltage V and pressure P are constant [7, 16, 17]. According to the requirements for selecting input factors, the experimental variables were selected, including temperature TL, permeation time h, and gas permeation concentration $G1$. The remaining factors remain unchanged. The influence of plasma nitriding technology parameters on the working surface hardness of the part is described in the general regression equation (1):

$$H = f(h, TL, G1) \quad (1)$$

where H is the hardness of the working surface (HV).

To study how the working hardness of the sample is affected by the plasma nitriding technology parameters, we designed a second-order experiment with 27 trials and used the software of the H4580 Eltrolab device to regulate the nitriding process [16]. The levels of the parameters are shown in Table I.

TABLE I. PARAMETER LEVELS OF THE EXPERIMENTAL DESIGN

Parameter			Level		
Name	**Symbol**	**Unit**	**(-1)**	**(0)**	**(+1)**
Temperature	TL	(°C)	510	530	550
Permeation time	h	h	4	6	8
Gas permeation concentration	$G1$	$(^{l}/_{h})$	4	6	8

The power is turned off at high voltage and low pressure to start the surface activation stage, which initiates the first heating process until the temperature reaches 250 to 300 °C. The second heating process follows until the temperature reaches the permeation temperature of 510 to 550 °C. The permeation period lasts from 4 to 8 h, depending on the experiment parameters, and then the automatic cooling phase begins. Experimental and control samples after permeation in each experiment are shown in Figure 1(b). The Vickers hardness measurement method (HV), according to the JIS Z 2244 - 2009 standard, with the FM-700e instrument, was used to test the microscopic hardness of the experimental sample, because the plasma nitriding layer on its surface is very thin (μm scale). The experiment sample measurement results are shown in Table II. We used the statistical software Minitab 21 to analyze the experimental results (Table II) with a full second order polynomial model [17, 19-21]. The results are shown in Table III. In Table III, we noted that the coefficients of $G1*G1$ and $h*TL$ have a P-Value greater than the significance level α=5%=0.05 (i.e. confidence interval CI < 95%), which means that these terms have no significant effect in the regression equation, so they were removed, and the experimental results were re-analyzed with other terms. The results are shown in Table IV.

TABLE II. EXPERIMENTAL RESULTS

Trial	h **(h)**	TL **(°C)**	$G1$ **(l/h)**	H **(HV)**
1	4	510	4	632.0
2	4	510	6	644.2
3	4	510	8	654.1
4	4	530	4	670.7
5	4	530	6	676.2
6	4	530	8	678.8
7	4	550	4	699.9
8	4	550	6	700.4
9	4	550	8	694.2
10	6	510	4	638.1
11	6	510	6	641.3
12	6	510	8	653.5
13	6	530	4	670.6
14	6	530	6	677.9
15	6	530	8	676.4
16	6	550	4	703.1
17	6	550	6	701.5
18	6	550	8	693.9
19	8	510	4	652.7
20	8	510	6	652.7
21	8	510	8	659.7
22	8	530	4	684.8
23	8	530	6	681.4
24	8	530	8	684.3
25	8	550	4	717.0
26	8	550	6	706.1
27	8	550	8	701.9

TABLE III. PRELIMINARY COEFFICIENTS OF THE REGRESSION EQUATION

Term	Coef	SE Coef	T-Value	P-Value	VIF
Constant	674.91	1.14	592.34	0.000	
h	5.006	0.527	9.49	0.000	1.00
TL	27.206	0.527	51.58	0.000	1.00
$G1$	1.550	0.527	2.94	0.009	1.00
h*h	4.361	0.914	4.77	0.000	1.00
TL*TL	-3.106	0.914	-3.40	0.003	1.00
G1*G1	0.128	0.914	0.14	0.890	1.00
$h*TL$	-0.358	0.646	-0.55	0.586	1.00
$h*G1$	-2.758	0.646	-4.27	0.001	1.00
$TL*G1$	-6.208	0.646	-9.61	0.000	1.00

TABLE IV. COEFFICIENTS OF THE REGRESSION EQUATION AFTER REMOVING THE NON-SIGNIFICANT TERMS

Term	Coef	SE Coef	T-Value	P-Value	VIF
Constant	674.993	0.920	734.00	0.000	
h	5.006	0.504	9.94	0.000	1.00
T□□	27.206	0.504	54.01	0.000	1.00
$G1$	1.550	0.504	3.08	0.006	1.00
$h*h$	4.361	0.872	5.00	0.000	1.00
$TL*TL$	-3.106	0.872	-3.56	0.002	1.00
$h*G1$	-2.758	0.617	-4.47	0.000	1.00
$TL*G1$	-6.208	0.617	-10.06	0.000	1.00

Analysis of Variance (ANOVA) was performed for the regression equation of the experimental results, with the option to remove the terms that have non-significant effect on the defined regression equation [17-20, 22, 23]. The analysis of ANOVA table (Table V) has all the P-Values less than α=5%, i.e. the parameters with a significant effect on the regression equation.

TABLE V. ANALYSIS OF VARIANCE

Source	DF	Adj SS	Adj MS	F-Value	P-Value
Model	7	14542.6	2077.5	454.93	0.000
Linear	3	13816.8	4605.6	1008.53	0.000
h	1	451.0	451.0	98.76	0.000
TL	1	13322.6	13322.6	2917.37	0.000
$G1$	1	43.2	43.2	9.47	0.006
Square	2	172.0	86.0	18.83	0.000
$h*h$	1	114.1	114.1	24.99	0.000
$TL*TL$	1	57.9	57.9	12.67	0.002
2-Way Interaction	2	553.8	276.9	60.64	0.000
$h*G1$	1	91.3	91.3	19.99	0.000
$TL*G1$	1	462.5	462.5	101.28	0.000
Error	19	86.8	4.6		
Total	26	14629.4			

By using statistical software, the result table of the regression coefficient evaluation parameters can be determined, as in Table VI. The parameters R^2 (R-squared), R^2-adj (R^2-adjusted), and R^2-pred (R^2-predicted) all have values larger than 90%, that is, the regression equation fits perfectly with the experimental data [24, 25]. The regression equation for working hardness H is written in natural form as follows:

$$H = 2726 - 6.44h + 10.52TL + 87.17G1 + 1.090h^2 - 0.00776TL^2 - 0.690h \times G1 - 0.1552TL \times G1 \quad (2)$$

TABLE VI. REGRESSION COEFFICIENT EVALUATION PARAMETERS

S	R-sq	R-sq(adj)	R-sq(pred)
2.13697	99.41%	99.19%	98.85%

III. RESULTS AND DISCUSSION

The influence of the input parameters on the output parameters is shown in Figure 2. Regression equation (2) and Figure 2 show that the permeation temperature TL has the greatest influence on hardness, while the permeation time h and the gas permeation concentration $G1$ have less influence.

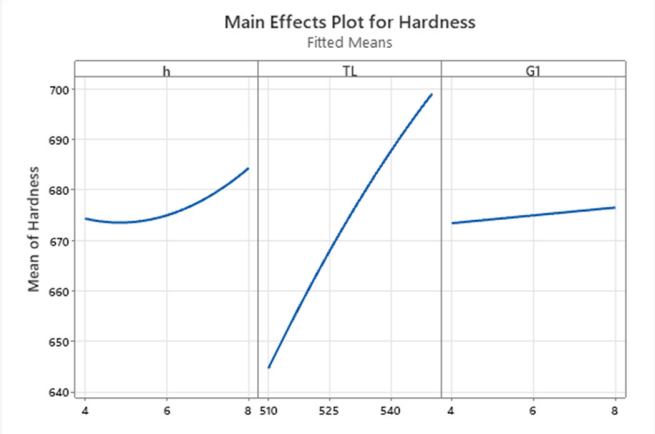

Fig. 2. Chart of the influence of technological parameters on hardness.

In Figure 2, corresponding to the three levels of each parameter, the software calculates the average value of the output response and represents it as a point. Consequentially, in order to find out the technological parameters that most affect the output value, it is possible to make a brief comment on the influence of the input parameters on the output parameter. With permeation time h, the effect on hardness is parabolic, with the minimum being near level (0), the effect chart goes from the interval value to the minimum and approaches the maximum value of 685 HV at the level area (+1) of the plan. With the permeation temperature TL, the effect on hardness is in the form of parabolic branches, with the smallest value being about 645 HV and the maximum value being about 700 HV, with no extremes in the planning space. Regarding the gas permeation concentration $G1$, the effect on hardness is linear, going from the minimum value at level (-1) and towards the maximum value at level (+1).

The Pareto chart in Figure 3, in addition to visualizing the influence of the coefficients on the result of the regression equation, also shows the influence of the technological parameters on the hardness of the working surface. Accordingly, the permeation temperature TL has the greatest influence on hardness, followed by the permeation time h, whereas the gas permeation concentration $G1$ has the least influence. The double interaction between permeation temperature TL and gas permeation concentration $G1$ and permeation time h also affects the surface hardness.

Figures 4-6 show more clearly the double interaction between the parameters. From these charts, the changing trend of hardness H is known when changing each pair of technological parameters. That is, when the permeation temperature TL and the penetration time h increase together, the working surface hardness H increases, but the effect of the permeation temperature TL is stronger (Figure 4).

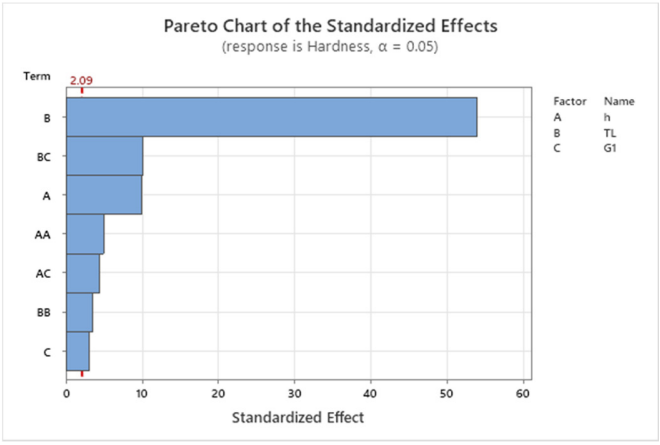

Fig. 3. Pareto chart with input parameters.

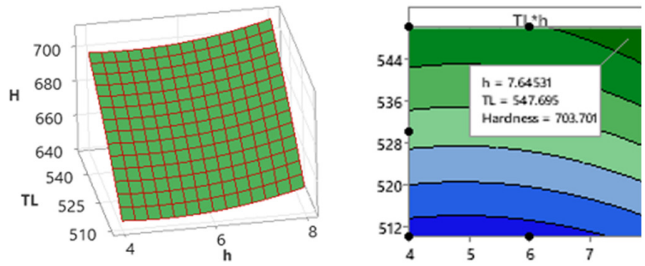

Fig. 4. Charts of interaction between permeation temperature and time to hardness.

Although the permeation time h and the gas permeation concentration $G1$ increase, making the hardness of the working surface H increase, in general, the effect is not much, as shown in (2) and Figure 5.

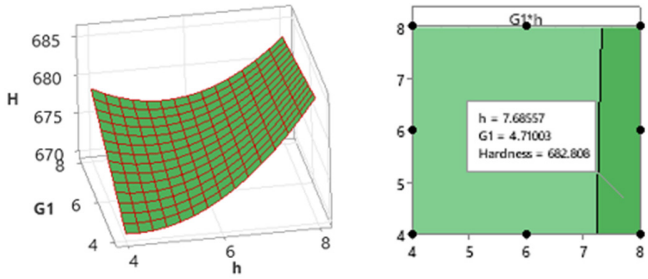

Fig. 5. Chart of interaction between gas permeation concentration and permeation time to hardness.

When the gas permeation concentration $G1$ and the permeation temperature TL increase, they make the hardness of the working surface H increase, but the effect of the permeation temperature is much larger, as shown in Figure 6.

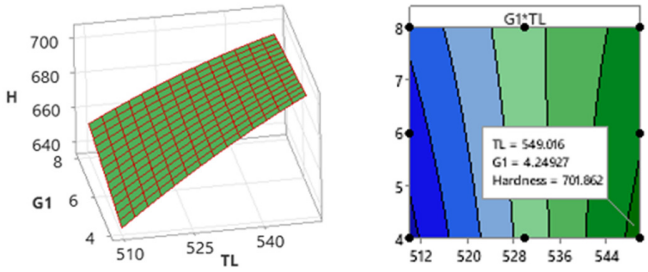

Fig. 6. Chart of interaction between gas permeation concentration and permeation time to hardness.

The above analysis shows that the permeation temperature TL has the greatest influence on hardness. This conclusion is in accordance with the results of [7, 16, 23].

IV. CONCLUSION

Research results on the influence of plasma nitriding technology parameters on the working surface hardness of machine parts made of 18ХГТ material, specifically, the pair of hypoid gears in the rear axle of light trucks manufactured in Vietnam, have been presented in the article. The regression function is set up with visual charts as a basis for analyzing the influence of temperature, time, and gas permeation concentration on the hardness of the gear working surface. The analysis shows that the permeation temperature TL has the greatest influence on hardness, while the permeation time h and the gas permeation concentration $G1$ have less influence. Specifically, in permeation temperature TL = 550 °C, permeation time h = 8 h and gas permeation concentration $G1$ = 4 l/h, the surface microhardness reaches 717.0 HV. The results of this study can be used when plasma nitrogen with different machine parts is made of 18ХГТ material or materials with equivalent chemical, mechanical, and physical properties. In following research, we will investigate how the plasma nitriding technology parameters affect the depth of the plasma nitriding layer of different machine parts made of 18ХГТ material or similar materials to get optimal results.

REFERENCES

[1] D. Pye, *Practical Nitriding and Ferritic Nitrocarburizing*. Materials Park, OH, USA: ASM International, 2003.

[2] *ISO/TR 22849:2011. Design recommendations for bevel gears.* ISO, 2011.

[3] D. Y. Chung, H. J. Kim, and H. N. Kim, "A Study on the Erosion Characteristics of the Micropulsed Plasma Nitrided Barrel of a Rifle," in *19th International Symposium of Ballistics*, Interlaken, Switzerland, May 2001.

[4] T. K. Hirsch, A. D. S. Rocha, F. D. Ramos, and T. R. Strohaecker, "Residual stress-affected diffusion during plasma nitriding of tool steels," *Metallurgical and Materials Transactions A*, vol. 35, no. 11, pp. 3523–3530, Nov. 2004, https://doi.org/10.1007/s11661-004-0189-2.

[5] U. Huchel and S. Strämke, *Pulsed Plasma Nitriding of Sintered Parts–Production Experiences*. Baesweiler, Germany: ELTRO GmbH, 2003.

[6] U. Huchel, *Pulsed Plasma Nitriding of Sintered Parts–Production Experiences*. Baesweiler, Germany: ELTRO GmbH, 2003.

[7] D. Vu, "Prediction of the Adhesion Strength of Coating in Plasma Spray Deposition," *Engineering, Technology & Applied Science Research*, vol. 13, no. 2, pp. 10367–10371, Apr. 2023, https://doi.org/10.48084/etasr.5673.

[8] L. Maldzinski, W. Liliental, G. Tymowski, and J. Tacikowski, "New possibilities for controlling gas nitriding process by simulation of growth kinetics of nitride layers," *Surface Engineering*, vol. 15, no. 5, pp. 377–384, Oct. 1999, https://doi.org/10.1179/026708499101516740.

[9] O. Ortac, "Microstructural and mechanical characterization of nitrogen ion implanted and plasma ion nitrided plastic injection mould steel," M. S. thesis, Izmir Institute of Technology, Izmir, Turkey, 2003.

[10] V. I. Dimitrov, G. Knuyt, L. M. Stals, J. D'Haen, and C. Quaeyhaegens, "Generalized Wagner's diffusion model of surface modification of materials by plasma diffusion treatment," *Applied Physics A*, vol. 67, no. 2, pp. 183–192, Aug. 1998, https://doi.org/10.1007/s003390050757.

[11] M. Yan, J. Yan, and T. Bell, "Numerical simulation of nitrided layer growth and nitrogen distribution in ε-Fe2-3N, γ'-Fe4N and α-Fe during pulse plasma nitriding of pure iron," *Modelling and Simulation in Materials Science and Engineering*, vol. 8, no. 4, Apr. 2000, https://doi.org/10.1088/0965-0393/8/4/307.

[12] J. Baranowska, *Plasma Nitriding and Plasma Immersion Ion Implantation*. Szczecin University of Technology, 2008.

[13] T. Belmonte, M. Gouné, and H. Michel, "Numerical modeling of interstitial diffusion in binary systems. Application to iron nitriding," *Materials Science and Engineering: A*, vol. 302, no. 2, pp. 246–257, Apr. 2001, https://doi.org/10.1016/S0921-5093(00)01830-X.

[14] M. Keddam, "Surface modification of the pure iron by the pulse plasma nitriding: Application of a kinetic model," *Materials Science and Engineering: A*, vol. 462, no. 1, pp. 169–173, Jul. 2007, https://doi.org/10.1016/j.msea.2006.02.459.

[15] M. B. Karamiş, "Some effects of the plasma nitriding process on layer properties," *Thin Solid Films*, vol. 217, no. 1, pp. 38–47, Sep. 1992, https://doi.org/10.1016/0040-6090(92)90603-9.

[16] H. K. Le, "A Study on the Influence of Plasma Nitriding Technology Parameters on the Working Surface Deformation of Hypoid Gears," *Engineering, Technology & Applied Science Research*, vol. 12, no. 6, pp. 9760–9765, Dec. 2022, https://doi.org/10.48084/etasr.5365.

[17] T. H. Le, V. B. Pham, and T. D. Hoang, "Surface Finish Comparison of Dry and Coolant Fluid High-Speed Milling of JIS SDK61 Mould Steel," *Engineering, Technology & Applied Science Research*, vol. 12, no. 1, pp. 8023–8028, Feb. 2022, https://doi.org/10.48084/etasr.4594.

[18] "Марочник сталей и сплавов онлайн - скачать PDF," *Metal Place*. https://metal.place/ru/wiki/18khgt.

[19] D. T. Do and N.-T. Nguyen, "Applying Cocoso, Mabac, Mairca, Eamr, Topsis and Weight Determination Methods for Multi-Criteria Decision Making in Hole Turning Process," *Strojnícky časopis - Journal of Mechanical Engineering*, vol. 72, no. 2, pp. 15–40, Nov. 2022.

[20] D. D. Trung, "Influence of Cutting Parameters on Surface Roughness in Grinding of 65G Steel," *Tribology in Industry*, vol. 43, no. 1, pp. 167–176, Mar. 2021, https://doi.org/10.24874/ti.1009.11.20.01.

[21] K. P. Bui, T. D. Duc, C. Ngo, and M. N. Dinh, "Research on Optimization of Plunge Centerless Grinding Process using Genetic Algorithm and Response Surface Method," *Research on Optimization of Plunge Centerless Grinding Process using Genetic Algorithm and Response Surface Method*, vol. 4, no. 3, pp. 207–211, 2015.

[22] V. C. Nguyen, T. D. Nguyen, and D. H. Tien, "Cutting Parameter Optimization in Finishing Milling of Ti-6Al-4V Titanium Alloy under MQL Condition using TOPSIS and ANOVA Analysis," *Engineering, Technology & Applied Science Research*, vol. 11, no. 1, pp. 6775–6780, Feb. 2021, https://doi.org/10.48084/etasr.4015.

[23] B. T. Danh and L. H. Ky, "Optimization of Technological Parameters when Plasma Nitriding the Gear Working Surface," *Engineering, Technology & Applied Science Research*, vol. 13, no. 3, pp. 11006–11010, Jun. 2023, https://doi.org/10.48084/etasr.5946.

[24] "Model summary table for Fit Regression Model," *Minitab*. https://support.minitab.com/en-us/minitab/21/help-and-how-to/statistical-modeling/regression/how-to/fit-regression-model/interpret-the-results/all-statistics-and-graphs/model-summary-table/.

[25] D. C. Montgomery, *Design and Analysis of Experiments*, 10th ed. Hoboken, NJ, USA: Wiley, 2019.